Physica **108A** (1981) 333–360 *North-Holland Publishing Co.*

QUANTUM-KINETIC EQUATIONS FOR TIME CORRELATION FUNCTIONS IN HIGHER-ORDER PERTURBATION THEORY

M.C.J. LEERMAKERS and L.G. SUTTORP

Instituut voor Theoretische Fysica, Universiteit van Amsterdam, Valckenierstraat 65, 1018 XE Amsterdam, The Netherlands

Received 12 March 1981

The memory kernel of the kinetic equation for the time correlation function of a quantum fluid is determined both in third order of the interaction strength and in the low-density approximation. The results are obtained with the help of a diagram representation for the kernel. The connexion with the kinetic theory for classical fluids is established.

1. Introduction

The properties of a nonequilibrium fluid may be studied with the help of the kinetic theory of time correlation functions. These functions are determined by specifying the memory kernel in the kinetic equation that governs their time evolution. For classical fluids a suitable formalism that permits the approximate evaluation of this kernel has been developed several years ago (for a review see ref. 1). The generalization of these methods to the case of quantum fluids was considered in a few recent papers[2,3]). In particular, the memory kernel was established for a normal quantum fluid in the weak-coupling approximation. In the long-time and large-distance limit this kernel reduces to that of the linearized Uehling–Uhlenbeck equation[4]) in which the scattering amplitude is replaced by its first Born approximation.

The purpose of the present paper is to extend the available results by employing higher-order perturbation theory for the evaluation of the memory kernel. An essential ingredient of the treatment will consist in the introduction of four-point diagrams that represent the various contributions to the kernel. With the use of this diagram representation we shall derive the memory kernel in third order of the interaction strength. In this order the kernel still has the same general form as the weak-coupling kernel, but with shifted energies and a generalized transition probability. Its relation to the kernel of the linearized Bogoliubov–Gurov[5]) equation will be established.

An alternative approach to the approximate evaluation of the memory kernel makes use of an expansion in the density. The low-density limit of the

0378–4371/81/0000–0000/$02.50

kernel will be obtained in the second part of this paper by a systematic calculation of the infinite set of perturbative contributions that can be represented by ladder diagrams. It will be shown that one arrives in this way at the quantummechanical version of the linearized Boltzmann equation, with a cross section given by the complete Born series.

In a final section the classical limit of the quantum-kinetic kernels derived in this paper will be examined in some detail.

2. Resume of kinetic theory

A many-particle system can be described by multiparticle density operators defined as[2,6])

$$f(1,\ldots,n;t) = (2\pi\hbar)^{-3n}\int \mathrm{d}r_1'\ldots\mathrm{d}r_n' \exp\left(-\frac{\mathrm{i}}{\hbar}p_1\cdot r_1'\ldots-\frac{\mathrm{i}}{\hbar}p_n\cdot r_n'\right)$$
$$\times \Psi^\dagger(r_n-\tfrac{1}{2}r_n';t)\ldots\Psi^\dagger(r_1-\tfrac{1}{2}r_1';t)\Psi(r_1+\tfrac{1}{2}r_1';t)\ldots\Psi(r_n+\tfrac{1}{2}r_n';t). \quad (1)$$

The integers i in the argument of f stand for r_i, p_i. The field operators Ψ and $\Psi^\dagger$ obey the usual (anti-) commutation relations. Their time dependence is governed by a Hamiltonian operator, which for particles interacting through a central potential $v(12) = v(|r_1 - r_2|)$ reads

$$H = \int \mathrm{d}1(p_1^2/2m)f(1;0) + \tfrac{1}{2}\int \mathrm{d}1\,\mathrm{d}2\, v(1,2)f(1,2;0), \quad (2)$$

with m the particle mass.

Time correlation functions may be defined by[2])

$$F_{mn}(1,\ldots,m,1',\ldots,n';t-t') = \langle\tfrac{1}{2}\{\delta f(1,\ldots,m;t),\delta f(1',\ldots,n';t')\}\rangle, \quad (3)$$

involving an anticommutator of the deviation function $\delta f = f - \langle f\rangle$; the angular brackets denote averaging in the grand-canonical ensemble. Instead of (3) we will use its Laplace transform defined as

$$F_{mn}(1,\ldots,m,1',\ldots,n';z) = -\mathrm{i}\int_0^\infty \mathrm{d}t\, \mathrm{e}^{\mathrm{i}zt} F_{mn}(1,\ldots,m,1',\ldots,n';t). \quad (4)$$

Kinetic theory is mainly concerned with the properties of the lowest-order time correlation function, in particular its time evolution, which is described by the equation[1,2])

$$[z - L_0(1)]F_{11}(1,1';z) = \tilde{F}_{11}(1,1') + \int \mathrm{d}2\,\Sigma(1,2;z)F_{11}(2,1';z). \quad (5)$$

Here $L_0(1) = -i(p_1/m) \cdot \nabla_{r_1}$ is the free-particle Liouville operator, $\tilde{F}_{11} = F_{11}(t = 0)$ the static two-particle correlation function, and Σ an integral kernel, which is to be calculated in a suitable approximation. Instead of Σ one may introduce a modified kernel

$$K(1, 1'; z) = \int d2\, \Sigma(1, 2; z)\tilde{F}_{11}(2, 1'), \tag{6}$$

which can be written as the sum of a static and a dynamical part, $K = K^{(s)} + K^{(d)}$. The static part is given by

$$K^{(s)}(1, 1') = \int d2\, L_I(1, 2)\tilde{F}_{21}(1, 2, 1'), \tag{7}$$

where the interaction operator L_I is defined by

$$L_I(1, 2) = 2i\hbar^{-1}v(1, 2) \sin[\tfrac{1}{2}\hbar\overleftarrow{\nabla}_{r_1} \cdot (\nabla_{p_1} - \nabla_{p_2})]. \tag{8}$$

The dynamical part can be written as[1,2])

$$K^{(d)}(1, 1'; z) = -\int d2\, d2'\, L_I(1, 2)L_I(1', 2')G_{22}(1, 2, 1', 2'; z), \tag{9}$$

with the auxiliary function

$$G_{22}(1, 2, 1', 2'; z) = F_{22}(1, 2, 1', 2'; z) - \int d3\, d3'\, F_{21}(1, 2, 3; z)F_{11}^{-1}(3, 3'; z)F_{12}(3', 1', 2'; z). \tag{10}$$

In performing calculations it will be convenient to work with the spatial Fourier transform $\bar{F}_{mn}$ of the functions F_{mn}. The eq. (3) with (4) and (1) can be represented in momentum space as

$$\begin{aligned}(2\pi)^3\delta\Big(\sum_{i=1}^{m} k_i + \sum_{j=1}^{n} k_j'\Big)\bar{F}_{mn}(p_1, k_1, \ldots, p_m, k_m, p_1', k_1', \ldots, p_n', k_n'; z) \\ = \int dr_1 \ldots dr_m\, dr_1' \ldots dr_n'\, e^{-ik_1 \cdot r_1 \ldots -ik_n' \cdot r_n'} F_{mn}(1, \ldots, m, 1', \ldots, n'; z) \\ = -i\int_0^\infty dt\, e^{izt}\langle\{\tfrac{1}{2}\{\delta\bar{f}(p_1, k_1, \ldots, p_m, k_m; t), \delta\bar{f}(p_1', k_1', \ldots, p_n', k_n'; 0)\}\rangle,\end{aligned} \tag{11}$$

where we defined the density operator $\bar{f}$ in momentum space by

$$\bar{f}(p_1, k_1, \ldots, p_n, k_n; t) = (2\pi\hbar)^{-3n}\Psi^\dagger(p_{n-}; t) \ldots \Psi^\dagger(p_{1-}; t)\Psi(p_{1+}; t) \ldots \Psi(p_{n+}; t), \tag{12}$$

with $\Psi(p) = \int \mathrm{d}r \exp[(-\mathrm{i}/\hbar)p \cdot r]\Psi(r)$ and $p_{i\pm} = p_i \pm \frac{1}{2}\hbar k_i$. Similarly we can define Fourier transforms of the kernels $K^{(s)}$ and $K^{(d)}$.

In the following we are mainly interested in the long-time and large-distance limit $k \to 0$, $z \to \mathrm{i}0$. In the $k \to 0$ limit $K^{(s)}$ is known to vanish[2]), since this kernel is antisymmetric under $k \leftrightarrow -k$. So we are left with the dynamical kernel only, which according to (9) is given by

$$K(p_1, 0, p_1', 0; z) = \sum_{\sigma,\sigma'=\pm 1} K^{\sigma\sigma'} = -(2\pi)^{-6}\hbar^{-2} \sum_{\sigma,\sigma'=\pm 1} \sigma\sigma' \times \int \mathrm{d}p_2 \, \mathrm{d}p_2' \, \mathrm{d}k \, \mathrm{d}k' \, v(k)v(k') L^{\sigma\sigma'}(p_1, p_2, p_1', p_2'; k, k') \times \bar{G}_{22}(p_1, k, p_2, -k, p_1', k', p_2', -k'; z). \tag{13}$$

Here $\bar{G}$ is the Fourier transform of G defined in (10):

$$\bar{G}_{22}(p_1, k, p_2, -k, p_1', k', p_2', -k'; z) = \bar{F}_{22}(p_1, k, p_2, -k, p_1', k', p_2', -k'; z) - \int \mathrm{d}p_3 \, \mathrm{d}p_3' \bar{F}_{21}(p_1, k, p_2, -k, p_3, 0; z)\bar{F}_{11}^{-1}(p_3, 0, p_3', 0; z) \times \bar{F}_{12}(p_3', 0, p_1', k', p_2', -k'; z), \tag{14}$$

while the translation operators $L^{\sigma\sigma'}$, following from (8), have the form

$$L^{\sigma\sigma'}(p_1, p_2, p_1', p_2'; k, k') = \exp\left[\tfrac{1}{2}\sigma\hbar k \cdot \left(\frac{\partial}{\partial p_1} - \frac{\partial}{\partial p_2}\right) + \tfrac{1}{2}\sigma'\hbar k' \cdot \left(\frac{\partial}{\partial p_1'} - \frac{\partial}{\partial p_2'}\right)\right]. \tag{15}$$

In the next sections K will be calculated both in lowest orders of perturbation theory with respect to the interaction strength and in the dilute-gas limit.

3. Diagrammatic method for the weak-coupling limit

The kernel K of the kinetic equation may be evaluated in successive orders of perturbation theory by employing the usual methods of many-body theory[7]). The time correlation functions $\bar{F}$ that determine K according to (13) with (14) are defined in terms of averaged anticommutators of density operators $\delta\bar{f}$. The latter are related to averaged temperature-ordered products, since their Lehmann representations contain a common weight function $\rho(\omega)$:

$$-\mathrm{i}\int_0^\infty \mathrm{d}t\, \mathrm{e}^{\mathrm{i}zt}\langle\tfrac{1}{2}\{\delta\bar{f}(1,\ldots,m;t),\delta\bar{f}(1',\ldots,n';0)\}\rangle$$

$$=\int_{-\infty}^{\infty}\mathrm{d}\omega\,\tfrac{1}{2}(\mathrm{e}^{-\beta\hbar\omega}+1)\frac{\rho(\omega)}{z-\omega}, \tag{16}$$

$$\tfrac{1}{2}\int_{-\beta\hbar}^{\beta\hbar}\mathrm{d}\tau\,\mathrm{e}^{\mathrm{i}\nu\tau}\langle T_\tau[\delta\bar{f}(1,\ldots,m;\tau)\delta\bar{f}(1',\ldots,n';0)]\rangle$$

$$=\int_{-\infty}^{\infty}\mathrm{d}\omega(\mathrm{e}^{-\beta\hbar\omega}-1)\frac{\rho(\omega)}{\mathrm{i}\nu-\omega}. \tag{17}$$

Here $\hbar^{-1}\tau$ is an inverse temperature variable, T_τ the ordering operator with respect to τ and ν a discrete variable that takes the values $2\pi n/\beta\hbar$, with $n=0,\pm1,\pm2,\ldots$. A convenient way to determine the time correlation functions $\bar{F}$ consists in evaluating the left-hand side of (17) by means of the finite-temperature perturbation formalism of many-body theory and carrying out an analytical continuation with respect to the variable $\mathrm{i}\nu$. The perturbation expansion for the average of an ordered product $T_\tau(\bar{f}\bar{f})$ of multiparticle density operators (12) leads to Feynman diagrams of the general form of fig. 1; the average of $T_\tau(\delta\bar{f}\delta\bar{f})$ is then represented by the subset of all connected diagrams, i.e. those diagrams in which at least one contraction between primed and unprimed external lines occurs.

In lowest-order perturbation theory the function $\bar{G}_{22}$ is given by its free-particle approximation. The leading term $\bar{F}_{22}$ in $\bar{G}_{22}$ can be represented then by diagrams as in fig. 1, with $m=n=2$ and without interactions[2]). In fig. 2 we have drawn as an example two diagrams in which all contractions connect primed and unprimed lines. In diagram a the pair of lines connecting p_{1+}, p_{2+}

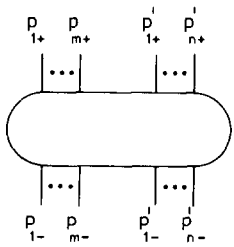

Fig. 1. General diagram for $\langle T_\tau[\delta\bar{f}(\boldsymbol{p}_1,\boldsymbol{k}_1,\ldots,\boldsymbol{p}_m,\boldsymbol{k}_m;\tau)\delta\bar{f}(\boldsymbol{p}'_1,\boldsymbol{k}'_1,\ldots,\boldsymbol{p}'_n,\boldsymbol{k}'_n;0)]\rangle$ or, after analytic continuation, for $\bar{F}_{mn}(\boldsymbol{p}_1,\boldsymbol{k}_1,\ldots,\boldsymbol{p}_m,\boldsymbol{k}_m,\boldsymbol{p}'_1,\boldsymbol{k}'_1,\ldots,\boldsymbol{p}'_n,\boldsymbol{k}'_n;z)$. The external momenta are $\boldsymbol{p}_{i\pm}=\boldsymbol{p}_i\pm\frac{1}{2}\hbar\boldsymbol{k}_i$ and $\boldsymbol{p}'_{i\pm}=\boldsymbol{p}'_i\pm\frac{1}{2}\hbar\boldsymbol{k}'_i$.

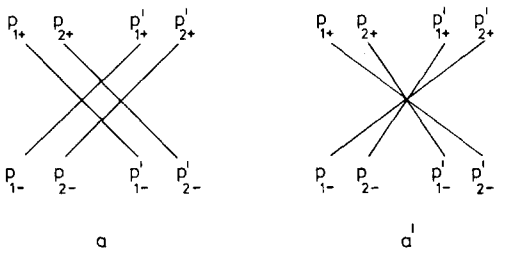

Fig. 2. Some zeroth-order diagrams for $\bar{G}_{22}$.

with p'_{1-}, p'_{2-} do not cross each other, while the other pair of lines has the same property. In diagram a' both pair of lines do cross.

According to the standard rules of many-body perturbation theory the contribution of diagram a to the left-hand side of (17) is

$$\tfrac{1}{2}\int_{-\beta\hbar}^{\beta\hbar} \mathrm{d}\tau\, \mathrm{e}^{\mathrm{i}\nu\tau}\,\delta(p_{1+}-p'_{1-})\delta(p_{2+}-p'_{2-})\delta(p'_{1+}-p_{1-})\delta(p'_{2+}-p_{2-})$$
$$\times G(p_{1+},\tau)G(p_{2+},\tau)G(p_{1-},-\tau)G(p_{2-},-\tau). \tag{18}$$

The propagator G is defined as[7])

$$G(p,\tau) = -\exp[-x(p)\tau][\tilde{n}(p)\theta(\tau)+\gamma n(p)\theta(-\tau)], \tag{19}$$

where $x(p)$ stands for the (reduced) energy $\hbar^{-1}[p^2/(2m)-\mu]$, with μ the chemical potential; furthermore $n(p)$ is the free-particle distribution function:

$$n(p) = \frac{(2\pi\hbar)^{-3}}{\exp[\beta\hbar x(p)]-\eta}, \tag{20}$$

(with $\eta = \pm 1$ for bosons or fermions) and $\tilde{n}(p) = 1+\gamma n(p)$, with $\gamma = \eta(2\pi\hbar)^3$. Carrying out the τ-integral in (18), using the auxiliary relation $\tilde{n}(p) = n(p)\exp[\beta\hbar x(p)]$ and performing the analytic continuation according to (16)–(17) we get the following contribution to the function $\bar{F}_{22}$:

$$\bar{F}_{22,a}(p_1,k_1,p_2,k_2,p'_1,k'_1,p'_2,k'_2;z)$$
$$= (2\pi\hbar)^3\delta(p_{1+}-p'_{1-})\delta(p_{2+}-p'_{2-})\delta(p'_{1+}-p_{1-})N(p_{1+},p_{2+},p_{1-},p_{2-};z); \tag{21}$$

here we introduced the abbreviation

$$N(p_1,p_2,p_3,p_4;z) = \frac{1}{2}\frac{n_1n_2\tilde{n}_3\tilde{n}_4+\tilde{n}_1\tilde{n}_2n_3n_4}{z-x_1-x_2+x_3+x_4}, \tag{22}$$

with $n_i = n(p_i)$ and $x_i = x(p_i)$.

The contributions to $\bar{F}_{22}$ from the remaining diagrams may be evaluated likewise. Most of these drop out, however, when the modified function $\bar{G}_{22}$ is considered[2]); in fact, the diagram identity of fig. 3 implies that only four

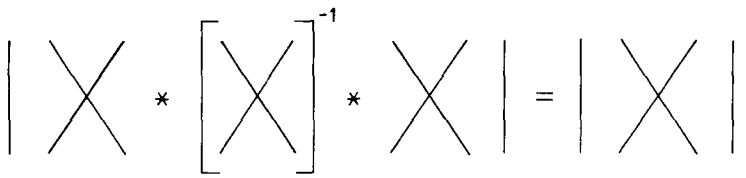

Fig. 3. Relation between subsidiary and main term of $\bar{G}_{22}$ (14) in lowest order. The subdiagrams represent $\bar{F}_{21}$, $\bar{F}_{11}^{-1}$ and $\bar{F}_{12}$, respectively, with labels as in fig. 1. (In fact, the first diagram is an abbreviation for four diagrams which differ only in a permutation of p_{1+}, p_{2+} and/or p_{1-}, p_{2-}; the third and fourth diagram must be interpreted similarly.)

diagrams contribute to $\bar{G}_{22}$, viz. those drawn in fig. 2, and two hybrids of these, with one noncrossing and one crossing pair of lines.

The partial kernels $K_a^{\sigma\sigma'}$ of diagram a follow according to (13) by applying to (21) the translation operators $L^{\sigma\sigma'}$. Noticing $L^{\sigma\sigma'}\boldsymbol{p}_1 = \boldsymbol{p}_1 + \frac{1}{2}\hbar\sigma\boldsymbol{k}$, etc., one may establish the relations

$$K_a^{\sigma\sigma'}(\boldsymbol{p}_1, \boldsymbol{0}, \boldsymbol{p}_1', \boldsymbol{0}; z) = -K_a^{-\sigma,-\sigma'}(\boldsymbol{p}_1, \boldsymbol{0}, \boldsymbol{p}_1', \boldsymbol{0}; -z). \tag{23}$$

If one uses the identity $(x + \mathrm{i}0)^{-1} - (x - \mathrm{i}0)^{-1} = -2\pi\mathrm{i}\delta(x)$ it follows that in the limit $z \to \mathrm{i}0$ the kernel $K = \Sigma_{\sigma\sigma'} K^{\sigma\sigma'}$ contains instead of N the function N_0 defined as

$$\begin{aligned} N_0(\boldsymbol{p}_1, \boldsymbol{p}_2, \boldsymbol{p}_3, \boldsymbol{p}_4) &= -\pi^{-1}\,\mathrm{Im}\, N(\boldsymbol{p}_1, \boldsymbol{p}_2, \boldsymbol{p}_3, \boldsymbol{p}_4; \mathrm{i}0) \\ &= \tfrac{1}{2}(n_1 n_2 \tilde{n}_3 \tilde{n}_4 + \tilde{n}_1 \tilde{n}_2 n_3 n_4)\delta(x_1 + x_2 - x_3 - x_4) \\ &= n_1 n_2 \tilde{n}_3 \tilde{n}_4 \delta(x_1 + x_2 - x_3 - x_4). \end{aligned} \tag{24}$$

With the notation $K(\boldsymbol{p}_1, \boldsymbol{p}_1') \equiv K(\boldsymbol{p}_1, \boldsymbol{0}, \boldsymbol{p}_1', \boldsymbol{0}; \mathrm{i}0)$ one finds for instance

$$\begin{aligned} K_a^{++}(\boldsymbol{p}_1, \boldsymbol{p}_1') + K_a^{--}(\boldsymbol{p}_1, \boldsymbol{p}_1') &= \mathrm{i}(2\pi\hbar)^{-2} \int \mathrm{d}\boldsymbol{p}_2\, \mathrm{d}\boldsymbol{p}_2'\, \mathrm{d}\boldsymbol{k}\, \mathrm{d}\boldsymbol{k}'\, v(\boldsymbol{k}) v(\boldsymbol{k}') \\ &\times \delta(\boldsymbol{k} + \boldsymbol{k}')\delta(\boldsymbol{p}_1 + \hbar\boldsymbol{k} - \boldsymbol{p}_1')\delta(\boldsymbol{p}_2 - \hbar\boldsymbol{k} - \boldsymbol{p}_2') N_0(\boldsymbol{p}_1, \boldsymbol{p}_2, \boldsymbol{p}_1', \boldsymbol{p}_2'). \end{aligned} \tag{25}$$

In the following we shall employ a diagram notation for the various contributions to the kernel K. In particular, the right-hand side of (25) will be represented by the diagram of fig. 4. Each (wavy) interaction line corresponds to a factor $v(\boldsymbol{k})$, while momentum-conserving delta functions are associated with the vertices (since overall momentum conservation is trivially satisfied, the corresponding delta function should be suppressed, as in (11)). Furthermore a factor $N_0(\boldsymbol{p}_1, \boldsymbol{p}_2, \boldsymbol{p}_3, \boldsymbol{p}_4)$ is represented by marked particle lines, see fig. 5. Finally, an integration over all internal lines is understood.

The diagram of fig. 4 has the virtue that it can be read off directly from fig. 2, and the prescription (13) for the evaluation of the kernel K. A more

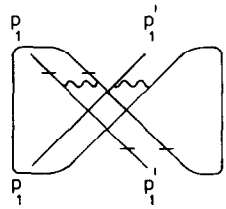

Fig. 4. Construction of the diagram representation for $K_a^{++} + K_a^{--}$.

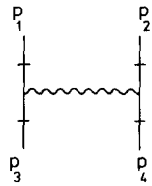

Fig. 5. Subdiagram with marks representing a factor N_0.

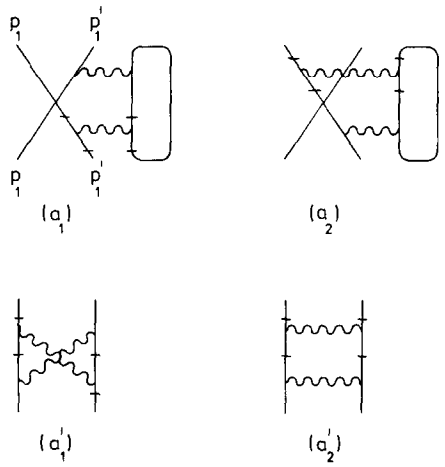

Fig. 6. Diagrams for the lowest-order kernel.

convenient but topologically equivalent way to represent it is given in fig. 6, diagram a_1. Likewise, the remaining contributions $K_a^{+-} + K_a^{-+}$ of diagram a give rise to diagram a_2 in fig. 6.

The diagram a' of fig. 2 may be treated in an analogous fashion. Once the diagram rules have been established there is no need to derive first the analytical expressions like (25); in fact, the diagrammatic representations a_1' and a_2' may be obtained straightforwardly from fig. 2.

With a suitable choice of integration variables the four diagrams of fig. 6

lead to the following expression for the kernel:

$$K_{a+a'}(p_1, p_1') = -i(2\pi)^{-2}\hbar^{-5}\int dp_2\, dp_3\, dp_4\, v_{13}^2\delta(p_1 + p_2 - p_3 - p_4)$$
$$\times \delta(x_1 + x_2 - x_3 - x_4)[\delta(p_1' - p_1) + \delta(p_1' - p_2)$$
$$- \delta(p_1' - p_3) - \delta(p_1' - p_4)]n_1 n_2 \tilde{n}_3 \tilde{n}_4, \tag{26}$$

where (24) has been used and the abbreviation $v_{ij} = v[(p_i - p_j)/\hbar]$ has been introduced; the contributions with $\delta(p_1' - p_i)$ $(i = 1, \ldots, 4)$ originate from the diagrams a_2, a_2', a_1, a_1', respectively.

The diagrams with one noncrossing and one crossing pair of lines, which contribute to $\bar{G}_{22}$ on a par with those of fig. 2, give rise to terms in the kernel that follow from (26) by replacing v_{13}^2 by $\eta v_{13} v_{14}$; as a consequence the complete second-order kernel is found from (26) by writing instead of v_{13}^2 the combination $v_{13}(v_{13} + \eta v_{14})$ or $\frac{1}{2}|T_W|^2$, with $T_W = v_{13} + \eta v_{14}$.

The kernel Σ follows from K by employing (6), which reads in Fourier space:

$$\Sigma(p, p') = \int dp'' K(p, p'')\tilde{\tilde{F}}_{11}^{-1}(0, p'', 0, p'). \tag{27}$$

Since the inverse static correlation function for free particles has the form

$$\tilde{\tilde{F}}_{11}^{-1}(0, p, 0, p') = \delta(p - p')/[n(p)\tilde{n}(p)], \tag{28}$$

one gets from (26) the final result for the weak-coupling kernel:

$$\Sigma(p_1, p_1') = -\tfrac{1}{2}i(2\pi)^{-2}\hbar^{-5}\int dp_2\, dp_3\, dp_4 |T_W|^2$$
$$\times \delta(p_1 + p_2 - p_3 - p_4)\delta(x_1 + x_2 - x_3 - x_4)$$
$$\times [\tilde{n}_1^{-1} n_2 \tilde{n}_3 \tilde{n}_4 \delta(p_1' - p_1) + n_1 \tilde{n}_2^{-1} \tilde{n}_3 \tilde{n}_4 \delta(p_1' - p_2)$$
$$- \tilde{n}_1 \tilde{n}_2 \tilde{n}_3^{-1} n_4 \delta(p_1' - p_3) - \tilde{n}_1 \tilde{n}_2 n_3 \tilde{n}_4^{-1} \delta(p_1' - p_4)]. \tag{29}$$

The expression between square brackets may be rewritten with the help of the identity $\tilde{n}_i^{-1} n_j \tilde{n}_k \tilde{n}_l = n_j \tilde{n}_k \tilde{n}_l - \gamma \tilde{n}_j n_k n_l$, which is valid if $x_i + x_j = x_k + x_l$. The right-hand side of this equality is the coefficient of $\delta n_i = n_i - n_i$ in the linearized form of the combination $n_i n_j \tilde{n}_k \tilde{n}_l - \tilde{n}_i \tilde{n}_j n_k n_l$ of nonequilibrium distribution functions n. Hence, the integral $\int dp_1' \Sigma(p_1, p_1')\delta n(p_1')$ is the linearized version of

$$\mathscr{C}_W(p_1) = -\tfrac{1}{2}i(2\pi)^{-2}\hbar^{-5}\int dp_2\, dp_3\, dp_4 |T_W|^2$$
$$\times \delta(p_1 + p_2 - p_3 - p_4)\delta(x_1 + x_2 - x_3 - x_4)(n_1 n_2 \tilde{n}_3 \tilde{n}_4 - \tilde{n}_1 \tilde{n}_2 n_3 n_4), \tag{30}$$

which is in fact the first Born approximation to the collision term of Uehling

and Uhlenbeck[4]). In the form (26) the kernel has been obtained previously in ref. 2. The derivation given here is meant as an introduction to the more elaborate calculation of the following sections. In particular the diagrammatic notation for the various contributions to the kinetic kernel will be very useful when higher-order perturbation theory is employed.

4. Third-order perturbation theory: the Bogoliubov–Gurov kernel

The evaluation of the contributions of higher-order perturbation theory to the kernel becomes increasingly complicated, although in principle the methods to be used are straightforward: one first derives the correlation functions $\bar{F}_{ij}$ (and hence $\bar{G}_{22}$) in the chosen order of perturbation theory via the finite-temperature formalism of many-body perturbation theory and an analytic continuation; subsequently the kernel is obtained through substitution of $\bar{G}_{22}$ in (13). In this section this general procedure will be applied to calculate the kernel in third order of the interaction. The final result will turn out to be still relatively simple, since a considerable number of terms that arise on applying the translation operators in (13) are found to cancel out.

The diagrams of the general form of fig. 1 that contribute to $\bar{F}_{22}$ up to first-order perturbation theory can be grouped in a number of classes. Firstly, the diagrams of fig. 2, but with dressed instead of bare propagators[7]), must be evaluated. The corresponding contributions to $\bar{F}_{22}$ follow from the results of the preceding section through the replacement of $x(\boldsymbol{p})$ by $\bar{x}(\boldsymbol{p})$ defined as:

$$\bar{x}(\boldsymbol{p}) = x(\boldsymbol{p}) + \hbar^{-1} \int \mathrm{d}\boldsymbol{p}' \left[v(\boldsymbol{0}) + \eta v\left(\frac{\boldsymbol{p}-\boldsymbol{p}'}{\hbar}\right)\right] n(\boldsymbol{p}'); \tag{31}$$

accordingly the distribution functions $n(\boldsymbol{p}) = n[x(\boldsymbol{p})]$ go over in $\bar{n}(\boldsymbol{p}) = n[\bar{x}(\boldsymbol{p})]$. Secondly, a number of diagrams occur that are of the same structure as in fig. 2, but with one interaction connecting the particle lines. These are of two types, called b and c in fig. 7, where only diagrams with pairs of noncrossing lines have been drawn. (The total number of diagrams of type b and c is 8 and 16, respectively.) Finally, diagrams are expected to show up in which only two instead of four contractions connect the external lines labelled by momenta with and without primes (see fig. 1). Most of these diagrams drop out, however, if the subsidiary term in $\bar{G}_{22}$ (14) is taken into account. To prove this one should employ the diagram identity of fig. 8 which is a generalization to first order of that of fig. 3. A few of the 16 diagrams that survive the cancellations have been drawn in fig. 9; later on it will turn out that the diagrams c and d are intimately related. The diagrams of figs. 7, 9 and the ensuing contributions to the kinetic kernel will be studied now in succession.

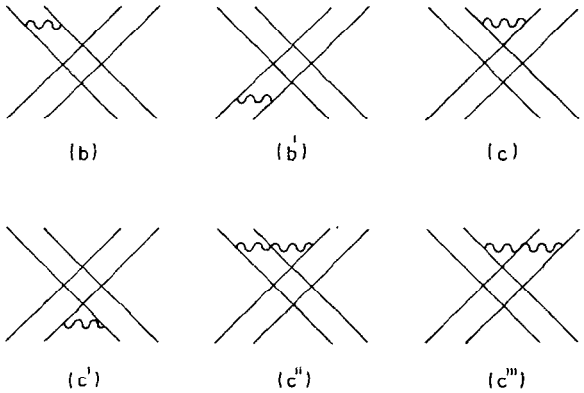

Fig. 7. Some first-order diagrams for $\bar{F}_{22}$.

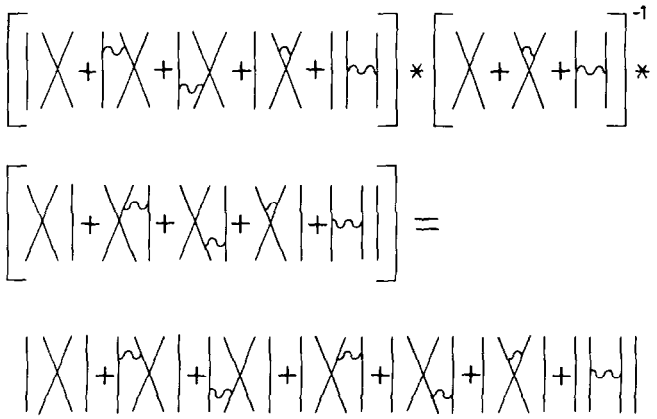

Fig. 8. Relation between terms of $\bar{G}_{22}$ in first order.

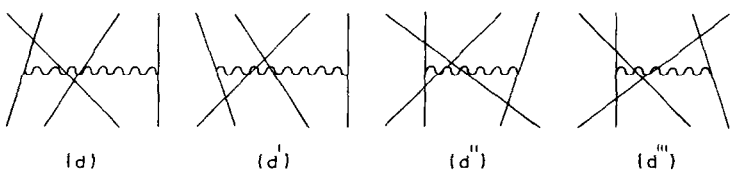

Fig. 9. Further diagrams for $\bar{G}_{22}$.

The term in $\bar{G}_{22}$ that is associated to diagram b in fig. 7 follows by applying the usual rules of many-body perturbation theory; one gets in this way

$$
\begin{aligned}
&-\hbar^2 \int \mathrm{d}q\, v(q)\delta(p_{1+}+\hbar q-p'_{1-})\delta(p_{2+}-\hbar q-p'_{2-})\delta(p'_{1+}-p_{1-}) \\
&\quad\times[M(p'_{1-},p'_{2-},p_{1+},p_{2+})N(p_{1+},p_{2+},p_{1-},p_{2-};z) \\
&\quad+M(p_{1+},p_{2+},p'_{1-},p'_{2-})N(p'_{1-},p'_{2-},p'_{1+},p'_{2+};z);
\end{aligned}
\tag{32}
$$

here M stands for the abbreviation

$$
M(p_1,p_2,p_3,p_4)=\frac{1+\gamma n_1+\gamma n_2}{x_1+x_2-x_3-x_4}=\frac{\frac{1}{2}(\gamma n_1+\tilde{n}_1)+\frac{1}{2}(\gamma n_2+\tilde{n}_2)}{x_1+x_2-x_3-x_4},
\tag{33}
$$

while N has been defined in (22).

The diagram b′ in fig. 7, which is connected to b by a reflection with respect to a horizontal line, leads to an analogous expression, with $p_{i+}\leftrightarrow p_{i-}$, $p'_{i+}\leftrightarrow p'_{i-}$, $z\leftrightarrow -z$ and a change of the overall sign. As a consequence the partial kernels following from b and b′ are connected by the relation (cf. (23))

$$
K_{\mathrm{b}}^{\sigma\sigma'}(p_1,\mathbf{0},p'_1,\mathbf{0};z)=-K_{\mathrm{b}'}^{-\sigma,-\sigma'}(p_1,\mathbf{0},p'_1,\mathbf{0};-z).
\tag{34}
$$

Hence, if the contributions of both diagrams are taken together the limit $z\to \mathrm{i}0$ is obtained by replacing the factors N in (32) by $-2\pi \mathrm{i}N_0$, as in the previous section. As an example we shall write down one of the combined partial kernels from the diagrams b and b′:

$$
\begin{aligned}
&K_{\mathrm{b}}^{++}(p_1,p'_1)+K_{\mathrm{b}'}^{--}(p_1,p'_1) \\
&\quad=-\mathrm{i}(2\pi)^{-5}\int \mathrm{d}p_2\,\mathrm{d}p'_2\,\mathrm{d}k\,\mathrm{d}k'\,\mathrm{d}q\, v(k)v(k')v(q) \\
&\qquad\times\delta(p_1+\hbar k+\hbar q-p'_1)\delta(p_2-\hbar k-\hbar q-p'_2)\delta(p'_1+\hbar k'-p_1) \\
&\qquad\times[M(p'_1,p'_2,p_1+\hbar k,p_2-\hbar k)N_0(p_1+\hbar k,p_2-\hbar k,p_1,p_2) \\
&\qquad+M(p_1+\hbar k,p_2-\hbar k,p'_1,p'_2)N_0(p'_1,p'_2,p'_1+\hbar k',p'_2-\hbar k')].
\end{aligned}
\tag{35}
$$

As in section 3 we want to represent the partial kernels by means of diagrams. To that end the rules given below (25) must be supplemented by a notation for the factor M. By convention the latter will be associated to a configuration consisting of an interaction line joining particle lines, two of which carry a mark (see fig. 10); the momenta of the marked lines appear as the last two variables in $M(p_1,p_2,p_3,p_4)$. The two terms in (35) can be represented now by the diagrams of fig. 11. It should be noticed that owing to the energy conserving delta function contained in N_0 it is immaterial which of the two possible interaction lines is chosen as the reference interaction with respect to which M is defined.

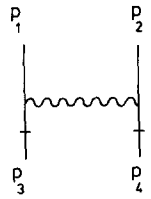

Fig. 10. Subdiagram with marks representing a factor M.

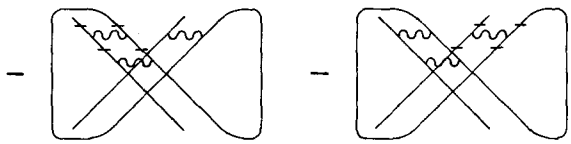

Fig. 11. Diagrammatic representation of $K_b^{++} + K_{b'}^{--}$.

The diagrams of fig. 11 can be deduced directly from those of fig. 7. A more transparent but equivalent way to represent them is shown in fig. 12, diagrams b_1 and b_2. The other diagrams in that figure represent the contributions $K_b^{--} + K_{b'}^{++}$ (see b_3, b_4), $K_b^{+-} + K_{b'}^{-+}$ (b_5, b_6) and $K_b^{-+} + K_{b'}^{+-}$ (b_7, b_8), which may be derived in an analogous fashion. These diagrams fall apart in four pairs. In fact, since the interpretation of a diagram does not change if it is drawn upside down, the diagrams b_1 and b_7 cancel, as do b_4 and b_8. Furthermore, b_2 and b_3 are identical, as are b_5 and b_6. To establish the last result use is made of the equality of p_1 and p_1' that is implied by momentum conservation along the particle line without vertices.

The kernel that follows from the diagrams b and b′ of fig. 7 is obtained now directly from b_2 and b_5 by choosing a suitable set of momentum integration variables. The kernel resulting from the diagrams b″ and b‴ that are the pendants of b and b′, but with two pairs of crossing particle lines, may be evaluated in a similar way. The final form for the kernel K_b that is associated to all four diagrams has the form

$$\begin{aligned} K_b(p_1, p_1') = &-2i(2\pi)^{-5}\hbar^{-9}\int dp_2\, dp_3\, dp_4\, dp_5\, dp_6\, v_{13}v_{35}v_{51} \\ &\times \frac{1+\gamma n_5+\gamma n_6}{x_1+x_2-x_5-x_6}\,\delta(p_1+p_2-p_5-p_6)\delta(p_1+p_2-p_3-p_4) \\ &\times \delta(x_1+x_2-x_3-x_4)[\delta(p_1'-p_1)+\delta(p_1'-p_2) \\ &-\delta(p_1'-p_3)-\delta(p_1'-p_4)]n_1n_2\bar{n}_3\bar{n}_4. \end{aligned} \tag{36}$$

The terms with $\delta(p_1'-p_1)$ and $\delta(p_1'-p_3)$ arise from b_5 and b_2, respectively, while those with $\delta(p_1'-p_2)$ and $\delta(p_1'-p_4)$ come from the diagrams b″ and b‴.

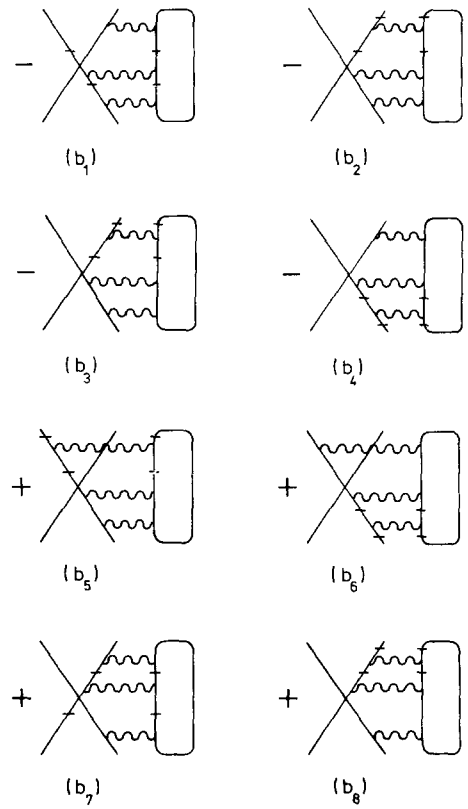

Fig. 12. Diagrams for $K_b + K_{b'}$.

The diagrams with one pair of crossing and one pair of noncrossing particle lines lead to a kernel of the same form as (36), with v_{13} replaced by ηv_{14}, so that the complete kernel due to all diagrams of type b is obtained by replacing in (36) the factor $v_{13}v_{35}v_{51}$ by $\frac{1}{2}(v_{13} + \eta v_{14})\,(v_{35} + \eta v_{45})v_{51}$.

Let us now consider the diagrams of type c in fig. 7. The diagram c itself gives the following contribution to the correlation function $\bar{G}_{22}$:

$$\hbar^2 \int \mathrm{d}\boldsymbol{q}\, v(\boldsymbol{q})\delta(\boldsymbol{p}_{1+} - \boldsymbol{p}'_{1-})\delta(\boldsymbol{p}_{2+} + \hbar\boldsymbol{q} - \boldsymbol{p}'_{2-})\delta(\boldsymbol{p}'_{1+} - \hbar\boldsymbol{q} - \boldsymbol{p}_{1-})$$
$$\times [M'(\boldsymbol{p}'_{1+}, \boldsymbol{p}_{2+}, \boldsymbol{p}_{1-}, \boldsymbol{p}'_{2-})N(\boldsymbol{p}_{1+}, \boldsymbol{p}_{2+}, \boldsymbol{p}_{1-}, \boldsymbol{p}_{2-}; z)$$
$$+ M'(\boldsymbol{p}_{1-}, \boldsymbol{p}'_{2-}, \boldsymbol{p}'_{1+}, \boldsymbol{p}_{2+})N(\boldsymbol{p}'_{1-}, \boldsymbol{p}'_{2-}, \boldsymbol{p}'_{1+}, \boldsymbol{p}'_{2+}; z)], \tag{37}$$

with

$$M'(\boldsymbol{p}_1, \boldsymbol{p}_2, \boldsymbol{p}_3, \boldsymbol{p}_4) = \gamma \frac{n_1 - n_4}{x_1 + x_2 - x_3 - x_4} = \frac{\frac{1}{2}(\gamma n_1 + \tilde{n}_1) - \frac{1}{2}(\gamma n_4 + \tilde{n}_4)}{x_1 + x_2 - x_3 - x_4}. \tag{38}$$

In evaluating the partial kernels corresponding to the various diagrams in fig. 7 one may use again relations like (34) so as to introduce delta functions expressing energy conservation. Like in the previous case the resulting expressions for the kernel can be represented by diagrams if one associates the factor $M'(p_1, p_2, p_3, p_4)$ to each of the configurations in fig. 13. Again it is found to be irrelevant which of the interaction lines in an actual diagram is adopted as the reference line for the identification of M'. The complete set of diagrams for the partial kernels $K_c^{\sigma\sigma'} + K_{\bar{c}'}^{-\sigma,-\sigma'}$ has been given in fig. 14. Inspection shows that the diagrams c_2, c_6 and c_3, c_5 cancel out, while c_1, c_4 and c_7, c_8 are pairwise identical.

The diagrams of type d given in fig. 9 may be evaluated in an analogous way. It turns out that some of the ensuing partial kernels exactly compensate contributions from diagrams of type c. To show this we shall briefly treat the first diagram of fig. 9, which yields the following term in $\bar{G}_{22}$:

$$\hbar^2 \int \mathrm{d}q\, v(q)\delta(p_{1+} - p'_{1-})\delta(p_{2+} + \hbar q - p_{1-})\delta(p'_{1+} - p_{2-})$$
$$\times [M'(p'_{2+}, p_{2+}, p_{1-}, p'_{2-})N(p_{1+}, p_{2+}, p_{1-}, p_{2-}; z)$$
$$+ M'(p_{1-}, p'_{2-}, p'_{2+}, p_{2+})N(p'_{1-}, p'_{2-}, p'_{1+}, p'_{2+}; z)], \tag{39}$$

with M' and N given in (38) and (22). The diagrammatic representation of the associated partial kernels is found straightforwardly by applying the same rules as above. As an example we give in fig. 15 the diagrams for $K_d^{++} + K_{\bar{d}'}^{--}$. By virtue of the same symmetry arguments as used before it can be shown that the first of these diagrams is equal to one of the diagrams representing $K_{d''}^{++} + K_{\bar{d}''}^{--}$, while the other compensates a diagram associated to $K_{c''}^{+-} + K_{\bar{c}''}^{-+}$. Since the diagrams of types c and d give rise to similar contributions it is convenient to combine the ensuing partial kernels in a single formula:

$$K_{c+d}(p_1, p'_1) = -2\mathrm{i}(2\pi)^{-2}\hbar^{-6} \int \mathrm{d}p_2\, \mathrm{d}p_3\, \mathrm{d}p_4\, \mathrm{d}p_5\, \mathrm{d}p_6$$
$$\times (v_{13} + \eta v_{14})(v_{13} + \eta v_{25})(v_{13} + \eta v_{35}) \frac{n_5 - n_6}{x_4 + x_5 - x_2 - x_6}$$
$$\times \delta(p_4 + p_5 - p_2 - p_6)\delta(p_1 + p_2 - p_3 - p_4)\delta(x_1 + x_2 - x_3 - x_4)$$
$$\times [\delta(p'_1 - p_1) + \delta(p'_1 - p_2) - \delta(p'_1 - p_3) - \delta(p'_1 - p_4)]n_1 n_2 \tilde{n}_3 \tilde{n}_4. \tag{40}$$

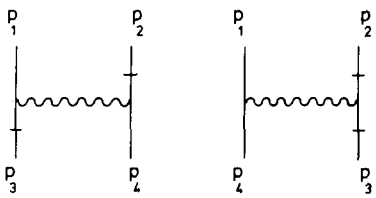

Fig. 13. Subdiagrams with marks representing a factor M'.

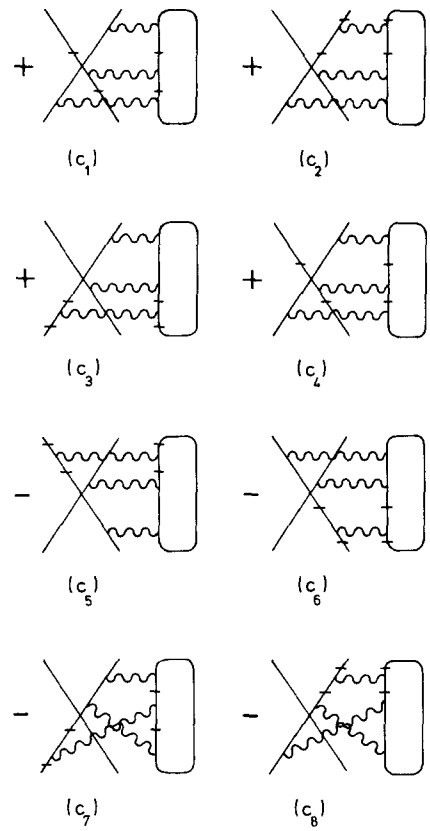

Fig. 14. Diagrams for $K_c + K_{c'}$.

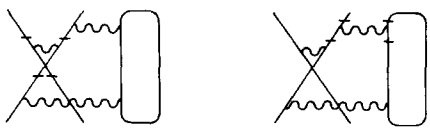

Fig. 15. The contribution $K_d^{++} + K_{d'}^{--}$ to the kernel.

Collecting the results (26) with (31), (36) and (40) we have found for the third-order kinetic kernel

$$K(p_1, p_1') = -\tfrac{1}{2}i(2\pi)^{-2}\hbar^{-5}\int dp_2\, dp_3\, dp_4 |T_{BG}|^2 \delta(p_1 + p_2 - p_3 - p_4)$$
$$\times \delta(\bar{x}_1 + \bar{x}_2 - \bar{x}_3 - \bar{x}_4)[\delta(p_1' - p_1) + \delta(p_1' - p_2)$$
$$- \delta(p_1' - p_3) - \delta(p_1' - p_4)]\bar{n}_1\bar{n}_2\tilde{\bar{n}}_3\tilde{\bar{n}}_4, \qquad (41)$$

with the abbreviation

$$T_{BG} = v_{13} + (2\pi)^{-3}\hbar^{-4}\int \mathrm{d}\boldsymbol{p}_5\,\mathrm{d}\boldsymbol{p}_6\, v_{35}v_{51}\frac{1+\gamma\bar{n}_5+\gamma\bar{n}_6}{\bar{x}_1+\bar{x}_2-\bar{x}_5-\bar{x}_6}$$
$$\times\,\delta(\boldsymbol{p}_1+\boldsymbol{p}_2-\boldsymbol{p}_5-\boldsymbol{p}_6)+\hbar^{-1}\int \mathrm{d}\boldsymbol{p}_5\,\mathrm{d}\boldsymbol{p}_6(v_{13}+\eta v_{25})(v_{13}+\eta v_{35})$$
$$\times\frac{\bar{n}_5-\bar{n}_6}{\bar{x}_4+\bar{x}_5-\bar{x}_2-\bar{x}_6}\,\delta(\boldsymbol{p}_4+\boldsymbol{p}_5-\boldsymbol{p}_2-\boldsymbol{p}_6)+\eta(3\leftrightarrow 4); \tag{42}$$

here $(3\leftrightarrow 4)$ stands for the preceding terms with labels 3 and 4 interchanged. Furthermore, notice that writing the kernel this compact way we mean it only to be valid up to third order, although higher-order terms are present now.

The kernel Σ that corresponds to K follows with (27) by using the inverse static correlation function up to first order in v

$$\tilde{\bar{F}}^{-1}(\mathbf{0},\boldsymbol{p},\mathbf{0},\boldsymbol{p}') = \frac{\delta(\boldsymbol{p}-\boldsymbol{p}')}{\bar{n}(\boldsymbol{p})\tilde{\bar{n}}(\boldsymbol{p}')}+\beta\left[v(\mathbf{0})+\eta v\left(\frac{\boldsymbol{p}-\boldsymbol{p}'}{\hbar}\right)\right]. \tag{43}$$

The third-order kernel Σ is then obtained as

$$\Sigma(\boldsymbol{p}_1,\boldsymbol{p}_1') = -\tfrac{1}{2}\mathrm{i}(2\pi)^{-2}\hbar^{-5}\int \mathrm{d}\boldsymbol{p}_2\,\mathrm{d}\boldsymbol{p}_3\,\mathrm{d}\boldsymbol{p}_4|T_{BG}|^2\delta(\boldsymbol{p}_1+\boldsymbol{p}_2-\boldsymbol{p}_3-\boldsymbol{p}_4)$$
$$\times\,\delta(\bar{x}_1+\bar{x}_2-\bar{x}_3-\bar{x}_4)[\tilde{\bar{n}}_1^{-1}\bar{n}_2\tilde{\bar{n}}_3\tilde{\bar{n}}_4\,\delta(\boldsymbol{p}_1'-\boldsymbol{p}_1)+\bar{n}_1\tilde{\bar{n}}_2^{-1}\tilde{\bar{n}}_3\tilde{\bar{n}}_4\delta(\boldsymbol{p}_1'-\boldsymbol{p}_2)$$
$$-\tilde{\bar{n}}_1\tilde{\bar{n}}_2\tilde{\bar{n}}_3^{-1}\bar{n}_4\delta(\boldsymbol{p}_1'-\boldsymbol{p}_3)-\tilde{\bar{n}}_1\tilde{\bar{n}}_2\bar{n}_3\tilde{\bar{n}}_4^{-1}\,\delta(\boldsymbol{p}_1'-\boldsymbol{p}_4)$$
$$+\beta\eta(v_{1'1}+v_{1'2}-v_{1'3}-v_{1'4})\bar{n}_1\,\bar{n}_2\tilde{\bar{n}}_3\tilde{\bar{n}}_4]. \tag{44}$$

To interpret this result one should notice that the expression between square brackets is related to the linearized form of the combination

$$\delta(\alpha_1+\alpha_2-\alpha_3-\alpha_4)(n_1n_2\tilde{n}_3\tilde{n}_4-\tilde{n}_1\tilde{n}_2n_3n_4), \tag{45}$$

where $\alpha_i = \alpha(\boldsymbol{p}_i)$ is given by (31), with $n(\boldsymbol{p}')$ replaced by $n(\boldsymbol{p}')$. In fact, writing $n_i = \bar{n}_i + \delta n_i$ one gets from (45) up to first order in δn_i:

$$\delta(\bar{x}_1+\bar{x}_2-\bar{x}_3-\bar{x}_4)(\tilde{\bar{n}}_1^{-1}\bar{n}_2\tilde{\bar{n}}_3\tilde{\bar{n}}_4\delta n_1+\bar{n}_1\tilde{\bar{n}}_2^{-1}\tilde{\bar{n}}_3\tilde{\bar{n}}_4\delta n_2$$
$$-\tilde{\bar{n}}_1\tilde{\bar{n}}_2\tilde{\bar{n}}_3^{-1}\bar{n}_4\delta n_3-\tilde{\bar{n}}_1\tilde{\bar{n}}_2\bar{n}_3\tilde{\bar{n}}_4^{-1}\delta n_4)$$
$$+\,\delta[\bar{x}_1+\bar{x}_2-\bar{x}_3-\bar{x}_4+\eta\hbar^{-1}\int \mathrm{d}\boldsymbol{p}_1'(v_{1'1}+v_{1'2}-v_{1'3}-v_{1'4})\delta n(\boldsymbol{p}_1')]$$
$$\times(\bar{n}_1\bar{n}_2\tilde{\bar{n}}_3\tilde{\bar{n}}_4-\tilde{\bar{n}}_1\tilde{\bar{n}}_2\bar{n}_3\bar{n}_4). \tag{46}$$

The factor with distribution functions in the second term may be rewritten as $\bar{n}_1\bar{n}_2\tilde{\bar{n}}_3\tilde{\bar{n}}_4[1-\exp\{\beta\hbar(\bar{x}_1+\bar{x}_2-\bar{x}_3-\bar{x}_4)\}]$. Using the energy delta function to eliminate $\bar{x}_1+\bar{x}_2-\bar{x}_3-\bar{x}_4$ and linearizing with respect to δn one finds for the

second term in (46)

$$\delta(\bar{x}_1+\bar{x}_2-\bar{x}_3-\bar{x}_4)\beta\eta\int \mathrm{d}p_1'(v_{1'1}+v_{1'2}-v_{1'3}-v_{1'4})\delta n(p_1')\bar{n}_1\bar{n}_2\bar{\tilde{n}}_3\bar{\tilde{n}}_4. \tag{47}$$

By comparing (46), (47) with (44) one concludes that $\int \mathrm{d}p_1'\Sigma(p_1, p_1')\delta n(p_1')$ is the linearized form of the collision term:

$$\mathscr{C}_{\mathrm{BG}}(p_1) = -\tfrac{1}{2}\mathrm{i}(2\pi)^{-2}\hbar^{-5}\int \mathrm{d}p_2\,\mathrm{d}p_3\,\mathrm{d}p_4|\mathscr{T}_{\mathrm{BG}}|^2\delta(p_1+p_2-p_3-p_4)$$
$$\times\,\delta(x_1-x_2-x_3-x_4)(n_1n_2\tilde{n}_3\tilde{n}_4-\tilde{n}_1\tilde{n}_2n_3n_4). \tag{48}$$

Here $\mathscr{T}_{\mathrm{BG}}$ is given by (42), with $\bar{n}_i$, $\bar{x}_i$ replaced by n_i, x_i; when $\mathscr{C}_{\mathrm{BG}}$ is linearized the difference between $\mathscr{T}_{\mathrm{BG}}$ and T_{BG} drops out since it is multiplied by $\bar{n}_1\bar{n}_2\bar{\tilde{n}}_3\bar{\tilde{n}}_4-\bar{\tilde{n}}_1\bar{\tilde{n}}_2\bar{n}_3\bar{n}_4$, which vanishes for momenta satisfying $\bar{x}_1+\bar{x}_2=\bar{x}_3+\bar{x}_4$. The collision term (48) has first been given by Bogoliubov and Gurov[5]). Its linearized form (44) has been obtained here by a systematic evaluation up to first-order perturbation theory of the diagrams for the four-point function $\bar{G}_{22}$ and the use of the representation (13) for the kinetic kernel. It should be noted here that in this order the kinetic kernel is still relatively simple. Effects of the finite life time of the excitations in the quantum fluid that complicate the kernel considerably show up only if at least second-order perturbation theory for $\bar{G}_{22}$ is employed.

5. Low-density limit: the quantummechanical Boltzmann kernel

In the previous sections we obtained a memory kernel by straightforwardly calculating successive orders of an expansion with respect to the coupling strength. In the present section we want to obtain a kinetic equation that is valid for a nondegenerate gas at low density n. In particular, we shall derive the memory kernel in the leading, second order of n. It will turn out that in this approximation the kernel can be evaluated up to all orders of the interaction strength.

To determine the order in n of a general diagram contributing to F_{mn} we note that the propagator (19) is proportional to n if $\tau \leqslant 0$ and of order n^0 for $\tau > 0$, since in the present approximation $n(p)$ is proportional to n and $\tilde{n}(p) = 1$. Hence, to select the dominant contribution in a diagram one should assign temperature variables τ to all interactions in such a way that the number of propagators bridging a nonpositive τ difference is minimal. In this way it can be shown that the function $\bar{F}_{11}$ starts off with terms of order n, while $\bar{F}_{21}$, $\bar{F}_{12}$ and $\bar{F}_{22}$ are of order n^2 and higher. As a consequence the subsidiary term in $\bar{G}_{22}$ can be neglected in the present approximation. In the

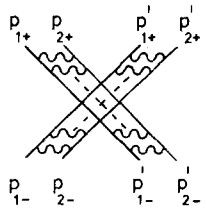

Fig. 16. General diagram with two ladders.

first term of $\bar{G}_{22}$ it turns out that only the diagrams consisting of two ladders, see fig. 16, contain terms of order n^2. In these diagrams all particle lines connect a primed and an unprimed momentum, the interactions being rungs forming two ladders. Besides the diagram explicitly drawn, there are three more diagrams that can be obtained from it by crossing the legs of one or both of the ladders. Since these are not essentially different, we will add their result at the end of our calculations.

To evaluate diagrams with many internal lines it is convenient to use the Fourier transform[7]) of the propagator (19)

$$G(p,\tau)=\frac{1}{\beta\hbar}\sum_{\omega}\frac{e^{-i\omega\tau}}{i\omega-x(p)}. \tag{49}$$

The frequency ω has discrete values, $\omega = n\pi/\beta\hbar$ and the summation is meant to be a sum over n, where n is even for bosons and odd for fermions.

By applying the normal many-body Feynman rules in momentum space, one obtains the contribution of fig. 16 to $\bar{G}_{22}$:

$$\begin{aligned}
&(-1)^{M+N}\hbar^{-M-N}(\beta\hbar)^{-M-N-3}(2\pi\hbar)^{-3M-3N-3}\int\prod_{k=0}^{M}\mathrm{d}q_k\prod_{l=0}^{N}\mathrm{d}q'_l\,\delta(\boldsymbol{P}_+-\boldsymbol{P}'_-)\\
&\quad\times\delta(q_0-p_{1-})\delta(q_M-p'_{1+})\delta(q'_0-p'_{1-})\\
&\quad\times\delta(q'_N-p_{1+})\prod_{i=1}^{M}v\left(\frac{q_i-q_{i-1}}{\hbar}\right)\prod_{j=1}^{N}v\left(\frac{q'_j-q'_{j-1}}{\hbar}\right)\\
&\quad\times\sum_{\Omega,\Omega'}\delta_{\Omega,\Omega'-\nu}\prod_{m=0}^{M}\sum_{\omega_m}[i\omega_m-x(q_m)]^{-1}[i(\Omega-\omega_m)-x(\boldsymbol{P}_--q_m)]^{-1}\\
&\quad\times\prod_{n=0}^{N}\sum_{\omega'_n}[i\omega'_n-x(q'_n)]^{-1}[i(\Omega'-\omega'_n)-x(\boldsymbol{P}'_--q'_n)]^{-1}.
\end{aligned}\tag{50}$$

Here M and N are the number of interactions along the two ladders, while $\boldsymbol{P}_\pm = p_{1\pm}+p_{2\pm}$ and $\boldsymbol{P}'_\pm = p'_{1\pm}+p'_{2\pm}$.

The summations over ω_m and ω'_n depend on particle statistics, while the

variables Ω and Ω', being in fact sums of two ω's, are always of the boson type. The manipulations needed to handle these frequency sums are explained in the appendix. The summations over ω_m and ω'_n can be carried out using (A.5), which reads in lowest order in the density:

$$\sum_{\omega} \frac{1}{\mathrm{i}\omega - x(q)} \frac{1}{\mathrm{i}(\omega - \Omega) + x(P-q)} = \frac{\beta\hbar}{\mathrm{i}\Omega - x(q) - x(P-q)}. \tag{51}$$

Next we are able to sum over Ω and Ω' with the help of (A.6), which in lowest order in the density gives

$$\begin{aligned}
&\sum_{\Omega} \prod_{m=0}^{M} \frac{1}{\mathrm{i}\Omega - x(q_m) - x(P-q_m)} \prod_{n=0}^{N} \frac{1}{\mathrm{i}(\Omega+\nu) - x(q'_n) - x(P'-q'_n)} \\
&\quad = -\beta\hbar(2\pi\hbar)^6 \sum_{m=0}^{M} \sum_{n=0}^{N} \prod_{\substack{\bar{m}=0 \\ (\bar{m}\neq m)}}^{M} \frac{1}{[x(q_m) + x(P-q_m) - x(q_{\bar{m}}) - x(P-q_{\bar{m}})]} \\
&\qquad \times \prod_{\substack{\bar{n}=0 \\ (\bar{n}\neq n)}}^{N} \frac{1}{[x(q'_n) + x(P'-q'_n) - x(q'_{\bar{n}}) - x(P'-q'_{\bar{n}})]} \\
&\qquad \times \frac{n(q_m)n(P-q_m) - n(q'_n)n(P'-q'_n)}{x(q_m) + x(P-q_m) - x(q'_n) - x(P'-q'_n) + \mathrm{i}\nu}.
\end{aligned} \tag{52}$$

Having dealt with the summations in (50) we perform an analytic continuation and arrive at the expression

$$\begin{aligned}
&\hbar^{-M-N}(2\pi\hbar)^{-3M-3N+3} \int \prod_{k=0}^{M} \mathrm{d}q_k \prod_{l=0}^{N} \mathrm{d}q'_l \, \delta(P_+ - P'_-) \\
&\quad \times \delta(q_0 - p_{1-})\delta(q_M - p'_{1+})\delta(q'_0 - p'_{1-})\delta(q'_N - p_{1+}) \prod_{i=1}^{M} v\left(\frac{q_i - q_{i-1}}{\hbar}\right) \\
&\quad \times \prod_{j=1}^{N} v\left(\frac{q'_j - q'_{j-1}}{\hbar}\right) \sum_{m=0}^{M} \sum_{n=0}^{N} N(q'_n, P'_- - q'_n, q_m, P_- - q_m; z) \\
&\quad \times \prod_{\substack{\bar{m}=0 \\ (\bar{m}\neq m)}}^{M} \bar{M}(q_m, P_- - q_m, q_{\bar{m}}, P_- - q_{\bar{m}}) \prod_{\substack{\bar{n}=0 \\ (\bar{n}\neq n)}}^{N} \bar{M}(q'_n, P'_- - q'_n, q'_{\bar{n}}, P'_- - q'_{\bar{n}}),
\end{aligned} \tag{53}$$

where N has been defined in (22) and $\bar{M}$ is just M as given by (33), with the numerator replaced by 1.

As before, in evaluating the kernel K it is convenient to consider together with fig. 16 the diagrams obtained by reflection with respect to a horizontal line. The corresponding contribution to $\bar{G}_{22}$ follows from (53) by an interchange of M and N. The expression (13) for the kernel contains two additional interaction potentials that we wish to treat on an equal footing with those appearing in (53). With the objective to adapt our notation to that fact we define

$$\tfrac{1}{2}(K^{\sigma\sigma'}_{MN} + K^{-\sigma,-\sigma'}_{MN}) = \hat{K}^{\pi\pi'}_{M'N'}, \tag{54}$$

with $\tau = \frac{1}{2}(1-\sigma)$ and $\tau' = \frac{1}{2}(1-\sigma')$, so that τ and τ' take the values 0 and 1. Furthermore, the relations $M' = M - \frac{1}{2}(\sigma - \sigma') + 1$ and $N' = N + \frac{1}{2}(\sigma - \sigma') + 1$ imply $M' \geqslant \tau - \tau' + 1$ and $N' \geqslant \tau' - \tau + 1$. In the limit $z \to \mathrm{i}0$ the newly defined partial kernel $\hat{K}$ can be written as

$$\begin{aligned}\hat{K}^{\tau\tau'}_{MN} = {} & \pi \mathrm{i}(-1)^{\tau+\tau'} \hbar^{-M-N} (2\pi\hbar)^{-3M-3N+3} \int \prod_{k=0}^{M} \mathrm{d}\boldsymbol{q}_k \prod_{l=0}^{N} \mathrm{d}\boldsymbol{q}'_l \, \mathrm{d}\boldsymbol{P} \\ & \times \delta(\boldsymbol{q}_0 - \boldsymbol{p}_1)\delta(\boldsymbol{q}_M - \boldsymbol{p}'_1)\delta(\boldsymbol{q}'_0 - \boldsymbol{p}'_1)\delta(\boldsymbol{q}'_N - \boldsymbol{p}_1) \prod_{i=1}^{M} v\left(\frac{\boldsymbol{q}_i - \boldsymbol{q}_{i-1}}{\hbar}\right) \\ & \times \prod_{j=1}^{N} v\left(\frac{\boldsymbol{q}'_j - \boldsymbol{q}'_{j-1}}{\hbar}\right) \sum_{m=\tau}^{M+\tau'-1} \sum_{n=\tau'}^{N+\tau-1} N_0(\boldsymbol{q}_m, \boldsymbol{P} - \boldsymbol{q}_m, \boldsymbol{q}'_n, \boldsymbol{P} - \boldsymbol{q}'_n) \\ & \times \prod_{\substack{\bar{m}=\tau \\ (\bar{m}\neq m)}}^{M+\tau'-1} \bar{M}(\boldsymbol{q}_m, \boldsymbol{P} - \boldsymbol{q}_m, \boldsymbol{q}_{\bar{m}}, \boldsymbol{P} - \boldsymbol{q}_{\bar{m}}) \prod_{\substack{\bar{n}=\tau' \\ (\bar{n}\neq n)}}^{N+\tau-1} \bar{M}(\boldsymbol{q}'_n, \boldsymbol{P} - \boldsymbol{q}'_n, \boldsymbol{q}'_{\bar{n}}, \boldsymbol{P} - \boldsymbol{q}'_{\bar{n}}).\end{aligned} \tag{55}$$

In comprehending the manipulations that follow presently it will be helpful to visualize the partial kernels (55) by means of the diagrams of fig. 17. These diagrams are related to those considered previously. However, in the present case a summation is implied over the labels of the momenta $\boldsymbol{q}_m$ and $\boldsymbol{q}'_n$ in the factors N_0, which were indicated by a dash in the earlier diagrams. From these summations are excluded the momenta belonging to the particle lines marked with a circle in fig. 17. The products of factors $\bar{M}$ contain apart from $\boldsymbol{q}_m$ and $\boldsymbol{q}'_n$ all other momenta $\boldsymbol{q}_{\bar{m}}$ and $\boldsymbol{q}'_{\bar{n}}$, again with the exception of the marked momenta.

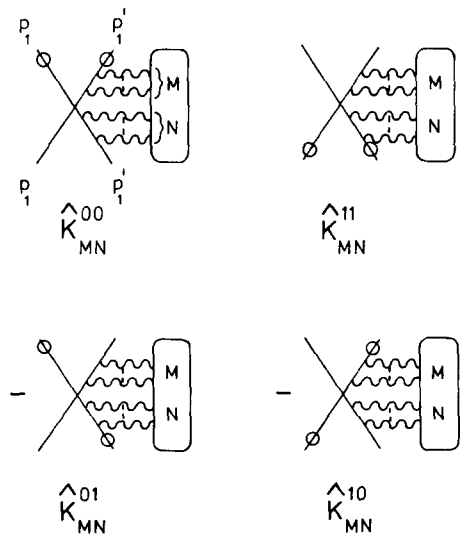

Fig. 17. The partial kernels $\hat{K}^{\tau\tau'}_{MN}$.

The complete kernel in the present approximation can be written now as a multiple sum over the partial kernels (55):

$$K = \sum_{\substack{M,N=0 \\ (M+N\geqslant 2)}}^{\infty} \left[\sum_{\tau,\tau'=0}^{1}{}' \hat{K}_{MN}^{\tau\tau'} \right]. \tag{56}$$

The summation over τ and τ' is restricted by the inequalities $1 - N \leqslant \tau - \tau' \leqslant M - 1$, as indicated by the prime. It will be shown now that many cancellations occur in the expression between square brackets. We shall consider first the case $M, N \geqslant 2$, for which the restriction on the summation over τ, τ' is of no consequence. Let us compare the diagrams for $\hat{K}_{MN}^{00}$ and $\hat{K}_{MN}^{01}$. They differ only in the position of the mark on p_1'. One concludes that in their sum all terms of $\hat{K}_{MN}^{00}$ drop out except for those with $n = 0$, since the latter is explicitly excluded in $\hat{K}_{MN}^{01}$. Similarly, only the terms with $m = M$ are left over of $\hat{K}_{MN}^{01}$, so that we may write

$$\hat{K}_{MN}^{00} + \hat{K}_{MN}^{01} = \hat{K}_{MN}^{00}(n = 0) + \hat{K}_{MN}^{01}(m = M). \tag{57}$$

Analogously it is seen that

$$\hat{K}_{MN}^{10} + \hat{K}_{MN}^{11} = \hat{K}_{MN}^{10}(n = 0) + \hat{K}_{MN}^{11}(m = M). \tag{58}$$

The right-hand sides of (57) and (58) can be handled in the same spirit:

$$\begin{aligned} &\hat{K}_{MN}^{00}(n = 0) + \hat{K}_{MN}^{10}(n = 0) = \hat{K}_{MN}^{00}(m = 0, n = 0), \\ &\hat{K}_{MN}^{01}(m = M) + \hat{K}_{MN}^{11}(m = M) = \hat{K}_{MN}^{11}(m = M, n = N). \end{aligned} \tag{59}$$

As a result we have found now for $M, N \geqslant 2$:

$$\sum_{\tau,\tau'=0}^{1} \hat{K}_{MN}^{\tau\tau'} = \hat{K}_{MN}^{00}(m = 0, n = 0) + \hat{K}_{MN}^{11}(m = M, n = N). \tag{60}$$

If M or N is less than 2 the possible values of τ and τ' are restricted. For instance, if $M = 1, N \geqslant 2$ the function $\hat{K}_{1N}^{10}$ does not exist. Nevertheless the reasoning given above can be repeated with minor changes. On a par with (57) one derives:

$$\hat{K}_{1N}^{00} + \hat{K}_{1N}^{01} = \hat{K}_{1N}^{00}(m = 0, n = 0) + \hat{K}_{1N}^{01}(m = 1). \tag{61}$$

Adding consecutively $\hat{K}_{1N}^{11}$ we again arrive at (60). The case $N = 1, M \geqslant 2$ is completely analogous, while for $M, N = 1$ eq. (60) is trivially satisfied.

The remaining terms in (56) are those with $M = 0$, $N \geqslant 2$, so that $\tau = 0$, $\tau' = 1$, and $N = 0$, $M \geqslant 2$, with $\tau' = 0$, $\tau = 1$. In the former case we may write

$$\hat{K}_{0N}^{01} = \sum_{n=1}^{N-1} \hat{K}_{0N}^{01}(m = 0, n), \tag{62}$$

while an analogous relation holds for $\hat{K}_{M0}^{10}$.

Combining (60) and (62) we obtain for the complete kernel (56):

$$K = 2\sum_{M,N=1}^{\infty} \hat{K}^{00}_{MN}(m=0, n=0) + 2\sum_{N=2}^{\infty}\sum_{n=1}^{N-1} \hat{K}^{01}_{0N}(m=0, n). \tag{63}$$

The two terms in (60) gave identical contributions, as did $\hat{K}^{10}_{M0}$ and $\hat{K}^{01}_{0N}$. A more explicit expression for the kernel follows by inserting (55) into (63). After a suitable change of integration variables the two terms in (63) can be written in a similar form. In fact, in the first term we introduce momenta $\boldsymbol{p}_2$, $\boldsymbol{p}_3$, $\boldsymbol{p}_4$ by writing $\boldsymbol{p}_2 = \boldsymbol{P} - \boldsymbol{p}_1$, $\boldsymbol{p}_4 = \boldsymbol{P} - \boldsymbol{p}_1'$ and inserting the factor $\int d\boldsymbol{p}_3 \delta(\boldsymbol{p}_1' - \boldsymbol{p}_3)$. In the second term the same momenta are introduced via $\boldsymbol{p}_2 = \boldsymbol{P} - \boldsymbol{p}_1$, $\boldsymbol{p}_3 = \boldsymbol{q}_n'$ and $\boldsymbol{p}_4 = \boldsymbol{P} - \boldsymbol{q}_n'$. Adding, moreover, the contribution of the three diagrams with crossed ladders we obtain as the low-density kernel

$$\begin{aligned} K(\boldsymbol{p}_1, \boldsymbol{p}_1') = &-\tfrac{1}{2}\mathrm{i}(2\pi)^{-2}\hbar^{-5}\int d\boldsymbol{p}_2\, d\boldsymbol{p}_3\, d\boldsymbol{p}_4 |T_B|^2 \delta(\boldsymbol{p}_1 + \boldsymbol{p}_2 - \boldsymbol{p}_3 - \boldsymbol{p}_4) \\ &\times \delta(x_1 + x_2 - x_3 - x_4)[\delta(\boldsymbol{p}_1' - \boldsymbol{p}_1) + \delta(\boldsymbol{p}_1' - \boldsymbol{p}_2) - \delta(\boldsymbol{p}_1' - \boldsymbol{p}_3) \\ &- \delta(\boldsymbol{p}_1' - \boldsymbol{p}_4)]n_1 n_2, \end{aligned} \tag{64}$$

where

$$\begin{aligned} T_B = &\, v\left(\frac{\boldsymbol{p}_1 - \boldsymbol{p}_3}{\hbar}\right) + \sum_{M=1}^{\infty}(2\pi)^{-3M}\hbar^{-4M}\int\prod_{k=1}^{M} d\boldsymbol{q}_k\, v\left(\frac{\boldsymbol{p}_1 - \boldsymbol{q}_1}{\hbar}\right) v\left(\frac{\boldsymbol{q}_1 - \boldsymbol{q}_2}{\hbar}\right) \\ &\cdots v\left(\frac{\boldsymbol{q}_M - \boldsymbol{p}_3}{\hbar}\right)\prod_{l=1}^{M}[x(\boldsymbol{p}_1) + x(\boldsymbol{p}_2) - x(\boldsymbol{q}_l) - x(\boldsymbol{p}_1 + \boldsymbol{p}_2 - \boldsymbol{q}_l)]^{-1} + \eta(3 \leftrightarrow 4). \end{aligned} \tag{65}$$

As in previous sections the terms proportional to η originated in the two diagrams with one crossed ladder, and the diagram with both ladders crossed gave rise to a doubling of the number of delta functions between square brackets. Note that T_B is just the complete Born series giving the amplitude for the scattering of two particles.

The low-density limit of the kernel Σ of the kinetic equation (5) is found by inserting $\tilde{\bar{F}}^{-1}(\boldsymbol{0}, \boldsymbol{p}, \boldsymbol{0}, \boldsymbol{p}') = \delta(\boldsymbol{p} - \boldsymbol{p}')/n(\boldsymbol{p})$ and (64) into (27):

$$\begin{aligned} \Sigma(\boldsymbol{p}_1, \boldsymbol{p}_1') = &-\tfrac{1}{2}\mathrm{i}(2\pi)^{-2}\hbar^{-5}\int d\boldsymbol{p}_2\, d\boldsymbol{p}_3\, d\boldsymbol{p}_4 |T_B|^2 \delta(\boldsymbol{p}_1 + \boldsymbol{p}_2 - \boldsymbol{p}_3 - \boldsymbol{p}_4) \\ &\times \delta(x_1 + x_2 - x_3 - x_4)[n_2\delta(\boldsymbol{p}_1' - \boldsymbol{p}_1) + n_1\delta(\boldsymbol{p}_1' - \boldsymbol{p}_2) \\ &- n_4\delta(\boldsymbol{p}_1' - \boldsymbol{p}_3) - n_3\delta(\boldsymbol{p}_1' - \boldsymbol{p}_4)]. \end{aligned} \tag{66}$$

The integral $\int d\boldsymbol{p}_1' \Sigma(\boldsymbol{p}_1, \boldsymbol{p}_1')\delta n(\boldsymbol{p}_1')$, with $\delta n(\boldsymbol{p}_i) = n(\boldsymbol{p}_i) - n(\boldsymbol{p}_i)$, is the linearized form of

$$\begin{aligned} \mathscr{C}_B = &-\tfrac{1}{2}\mathrm{i}(2\pi)^{-2}\hbar^{-5}\int d\boldsymbol{p}_2\, d\boldsymbol{p}_3\, d\boldsymbol{p}_4 |T_B|^2 \delta(\boldsymbol{p}_1 + \boldsymbol{p}_2 - \boldsymbol{p}_3 - \boldsymbol{p}_4) \\ &\times \delta(x_1 + x_2 - x_3 - x_4)(n_1 n_2 - n_3 n_4), \end{aligned} \tag{67}$$

which is the collision term of the quantummechanical Boltzmann equation.

6. The classical limit

The classical limit of the quantummechanical kinetic kernels derived in the previous sections is obtained by taking the limit $\hbar \to 0$. However, these kernels all contain inverse powers of $\hbar$, both explicitly and implicitly in the Fourier-transformed potentials. As a consequence, the study of the classical limit requires some care. In the following the three kinetic kernels given before will be considered consecutively.

The kinetic kernel (26) in the weak-coupling limit contains the free-particle distribution function $n(\boldsymbol{p})$, which in the classical limit reduces to $nf_0(\boldsymbol{p})$, with n the density and $f_0(\boldsymbol{p})$ the Maxwellian distribution; correspondingly, the function $\tilde{n}(\boldsymbol{p})$ can be put equal to 1. Furthermore, we choose new integration variables in such a way that the arguments of the Fourier-transformed potentials become of order $\hbar^0$. This is achieved by replacing $\boldsymbol{p}_3$ by $\boldsymbol{q} = (\boldsymbol{p}_3 - \boldsymbol{p}_1)/\hbar$. The kernel K given in (26) then becomes:

$$K^{\mathrm{cl}}(\boldsymbol{p}_1, \boldsymbol{p}_1') = -\mathrm{i}(2\pi)^{-2} n^2 \lim_{\hbar \to 0} \hbar^{-2} \int \mathrm{d}\boldsymbol{q}\, \mathrm{d}\boldsymbol{p}_2 [v(\boldsymbol{q})]^2 \delta[\boldsymbol{q} \cdot (\boldsymbol{p}_1 - \boldsymbol{p}_2)/m + \hbar q^2/m]$$
$$\times [\delta(\boldsymbol{p}_1' - \boldsymbol{p}_1) + \delta(\boldsymbol{p}_1' - \boldsymbol{p}_2) - \delta(\boldsymbol{p}_1' - \boldsymbol{p}_1 - \hbar\boldsymbol{q})$$
$$- \delta(\boldsymbol{p}_1' - \boldsymbol{p}_2 + \hbar\boldsymbol{q})] f_0(\boldsymbol{p}_1) f_0(\boldsymbol{p}_2). \tag{68}$$

The complete quantummechanical kernel in the weak-coupling limit follows from (26) by replacing v_{13}^2 by $\frac{1}{2}(v_{13} + \eta v_{14})^2$. However, in the classical limit the mixed terms $v_{13}\, v_{14}$ drop out. This is seen by introducing new integration variables such that both v_{13} and v_{14} contain arguments of order 1, in other words, by writing $\boldsymbol{q} = (\boldsymbol{p}_3 - \boldsymbol{p}_1)/\hbar$ and $\boldsymbol{q}' = (\boldsymbol{p}_4 - \boldsymbol{p}_1)/\hbar$; this change of variables leads to an integral expression that is of order $\hbar^3$ as compared to (68).

When the delta functions containing $\hbar$ in (68) are expanded in powers of $\hbar$ the leading term of the integral is found to be of order $\hbar^2$, since the contribution proportional to $\hbar$ drops out on account of the antisymmetry of the integrand under inversion of $\boldsymbol{q}$. After some partial integrations K^{cl} gets the form:

$$K^{\mathrm{cl}}(\boldsymbol{p}_1, \boldsymbol{p}_1') = -\tfrac{1}{2}\mathrm{i}(2\pi)^{-2} n^2 \nabla_{\boldsymbol{p}_1} \nabla_{\boldsymbol{p}_1'} : \int \mathrm{d}\boldsymbol{q}\, \boldsymbol{q}\boldsymbol{q} [v(\boldsymbol{q})]^2$$
$$\times \int \mathrm{d}\boldsymbol{p}_2\, \delta[\boldsymbol{q} \cdot (\boldsymbol{p}_1 - \boldsymbol{p}_2)/m] [\delta(\boldsymbol{p}_1' - \boldsymbol{p}_1) - \delta(\boldsymbol{p}_1' - \boldsymbol{p}_2)] f_0(\boldsymbol{p}_1) f_0(\boldsymbol{p}_2).$$

The corresponding kernel Σ^{cl} as defined by (27) follows by taking the classical

limit of the inverse static correlation function (28):

$$\Sigma^{\mathrm{cl}}(p, p') = K^{\mathrm{cl}}(p, p')/[nf_0(p')]. \tag{70}$$

As expected, the weak-coupling kernel Σ thus reduces in the classical approximation to the linearized version of the Landau collision term[8-10]).

Let us consider now the third-order kernel (41) with (42). The distribution functions $\bar{n}(p)$ again go over into $nf_0(p)$ in the classical limit; however, the density $n = n(\mu, T)$ now includes a first-order correction due to the interaction, as follows from the expression for $\bar{x}$ in (31). On the other hand, the difference between $\bar{x}$ and x in the energy-conserving delta function in (41) has no consequence in the classical limit: the term with $v(\mathbf{0})$ drops out, while the other term gives a negligible contribution for $\hbar \to 0$. To derive the classical limit of the partial kernels arising from each of the terms in $|T_{\mathrm{BG}}|^2$ one introduces new integration variables as before. It turns out that only the following terms in $|T_{\mathrm{BG}}|^2$ contribute for $\hbar \to 0$:

$$\begin{aligned} &v_{13}^2 + 2(2\pi)^{-3}\hbar^{-4}\int \mathrm{d}p_5\,\mathrm{d}p_6\, v_{13}v_{35}v_{51}(x_1 + x_2 - x_5 - x_6)^{-1}\delta(p_1 + p_2 - p_5 - p_6) \\ &\quad + 2\hbar^{-1}\int \mathrm{d}p_5\,\mathrm{d}p_6\, v_{13}^3(n_5 - n_6)(x_4 + x_5 - x_2 - x_6)^{-1} \\ &\quad \times \delta(p_4 + p_5 - p_2 - p_6) + (3 \leftrightarrow 4). \end{aligned} \tag{71}$$

As a consequence the third-order kernel becomes

$$\begin{aligned} K^{\mathrm{cl}}(p_1, p_1') = &-\mathrm{i}(2\pi)^{-2}n^2 \lim_{\hbar\to 0} \hbar^{-2}\int \mathrm{d}q\,\mathrm{d}p_2\,\delta[q\cdot(p_1 - p_2)/m + \hbar q^2/m] \\ &\times [\delta(p_1' - p_1) + \delta(p_1' - p_2) - \delta(p_1' - p_1 - \hbar q) \\ &- \delta(p_1' - p_2 + \hbar q)]f_0(p_1)f_0(p_2)\Big\{[v(q)]^2 + 2(2\pi)^{-3}\hbar^{-1} \\ &\times \int \mathrm{d}q' v(q)v(q')v(q + q')[q'\cdot(p_1 - p_2)/m - \hbar q'^2/m]^{-1} \\ &+ 2\hbar^{-1}n\int \mathrm{d}p_5[v(q)]^3[f_0(p_5) - f_0(p_5 - \hbar q)][q\cdot(p_5 - p_2)/m]^{-1}\Big\}. \end{aligned} \tag{72}$$

As in the second-order kernel we now expand the integrand in powers of $\hbar$. The first term between square brackets then leads again to (69). In the second term we use the symmetry of the integrand under the transformations $q, q' \leftrightarrow -q, -q'$ and $q' \leftrightarrow -q - q'$, while in the third term the symmetry with respect to $q \leftrightarrow -q$ is employed. A number of partial integrations then yield

$$K^{cl}(p_1, p_1') = -\tfrac{1}{2}i(2\pi)^{-2}n^2\nabla_{p_1}\nabla_{p_1'}:\int dq\, dp_2\, qq\delta[q\cdot(p_1-p_2)/m]$$
$$\times[\delta(p_1'-p_1)-\delta(p_1'-p_2)]f_0(p_1)f_0(p_2)\Big\{[v(q)]^2$$
$$-2(2\pi)^{-3}\int dq'\, v(q)v(q')v(q+q')(q+q')\cdot\nabla_{p_1}[m/q'\cdot(p_1-p_2)]$$
$$+2n\beta[v(q)]^3\int dp_5\, f_0(p_5)q\cdot p_5/q\cdot(p_1-p_5)\Big\}. \tag{73}$$

To obtain the kernel Σ^{cl} one uses the classical limit of the inverse static correlation function (43). The terms with βv in (43) do not contribute in the classical limit; for the first term this follows from the identity $\int dp_1' K^{cl}(p_1, p_1') = 0$, while the second term gives rise to extra factors $\hbar$ after a change of integration variables. Hence, the kernel Σ^{cl} is connected to K^{cl} through (70), as before. The resulting expression for Σ^{cl} is identical to the kernel obtained in a purely classical framework, as it should be. The latter may be derived by evaluating the terms of order v^2 and v^3 in the classical Boltzmann and Choh–Uhlenbeck[11]) kinetic kernels as given in ref. 12.

The classical limit of the quantummechanical Boltzmann kernel (64) with (65) is obtained easily when the differential cross section $d\sigma/d\Omega = m^2/(32\pi^2\hbar^4)|T_B|^2$ for the scattering process $p_1 + p_2 \to p_3 + p_4$ of identical particles is introduced. In the limit $\hbar \to 0$ the quantummechanical cross section reduces to its classical counterpart. Choosing furthermore as integration variables instead of p_3 the length and polar angles of the relative momentum $p_3 - p_4$ one finds immediately the well-known linearized classical Boltzmann kernel:

$$K^{cl}(p_1, p_1') = -in^2\int dp_2\, d\Omega(|p_1-p_2|/m)\, d\sigma/d\Omega$$
$$\times[\delta(p_1'-p_1)+\delta(p_1'-p_2)-\delta(p_1'-p_3)-\delta(p_1'-p_4)]f_0(p_1)f_0(p_2). \tag{74}$$

The kernel Σ^{cl} again follows by applying (70), since in the classical limit the inverse static correlation function $\tilde{F}^{-1}$ reduces to $\delta(p-p')/nf_0(p)$ for a dilute fluid.

Acknowledgements

This investigation is part of the research programme of the "Stichting voor Fundamenteel Onderzoek der Materie (FOM)", which is financially supported by the "Nederlandse Organisatie voor Zuiver-Wetenschappelijk Onderzoek (Z.W.O.)".

Appendix

Evaluation of frequency sums

In this appendix we shall perform some summations that are needed in section 5. To that end we consider the expression

$$I = \sum_{\omega} \left[\prod_{j=1}^{M} (\mathrm{i}\omega - a_j) \prod_{k=1}^{N} (\mathrm{i}\omega + \mathrm{i}\nu - b_k) \right]^{-1}, \tag{A.1}$$

where $e^{i\beta\hbar\nu} = 1$ and $e^{i\beta\hbar\omega} = \eta$. The summation can be turned into an integral along a contour around the imaginary axis[7]):

$$I = \frac{\eta\beta\hbar}{2\pi\mathrm{i}} \int_C \frac{\mathrm{d}z}{e^{\beta\hbar z} - \eta} \left[\prod_{j=1}^{M} (z - a_j) \prod_{k=1}^{N} (z + \mathrm{i}\nu - b_k) \right]^{-1}. \tag{A.2}$$

The products of z-dependent denominators may be rewritten with the use of relations of the type:

$$\prod_{j=1}^{M} (z - a_j)^{-1} = \sum_{j=1}^{M} \left[\prod_{l(\neq j)=1}^{M} (a_j - a_l)(z - a_j) \right]^{-1}. \tag{A.3}$$

If the contour is deformed so that it encircles the real axis, the integral can easily be calculated:

$$\begin{aligned} I = &- \beta\hbar\eta \sum_{j=1}^{M} \sum_{k=1}^{N} \left[\prod_{l(\neq j)=1}^{M} (a_j - a_l) \prod_{m(\neq k)=1}^{N} (b_k - b_m)(a_j - b_k + \mathrm{i}\nu) \right]^{-1} \\ &\times [(e^{\beta\hbar a_j} - \eta)^{-1} - (e^{\beta\hbar b_k} - \eta)^{-1}]. \end{aligned} \tag{A.4}$$

In section 5 the integral I is needed in two special cases. In the first case one has $M = N = 1$ and $a_1 = x(p_1)$, $b_1 = -x(\bar{p}_1)$. Then (A.4) can be written as

$$I = -\beta\hbar[x(p_1) + x(\bar{p}_1) + \mathrm{i}\nu]^{-1}[1 + \gamma n(p_1) + \gamma n(\bar{p}_1)]. \tag{A.5}$$

In the other case one has $\eta = 1$, $a_j = x(p_j) + x(\bar{p}_j)$ and $b_k = x(q_k) + x(\bar{q}_k)$. Eq. (A.4) then gives

$$\begin{aligned} I = &- \beta\hbar \sum_{j=1}^{M} \sum_{k=1}^{N} \left\{ \prod_{l(\neq j)=1}^{M} [x(p_j) + x(\bar{p}_j) - x(p_l) - x(\bar{p}_l)] \right. \\ &\times \prod_{m(\neq k)=1}^{N} [x(q_k) + x(\bar{q}_k) - x(q_m) - x(\bar{q}_m)] \\ &\left. \times [x(p_j) + x(\bar{p}_j) - x(q_k) - x(\bar{q}_k) + \mathrm{i}\nu] \right\}^{-1} \\ &\times \left[\frac{\gamma^2 n(p_j) n(\bar{p}_j)}{1 + \gamma n(p_j) + \gamma n(\bar{p}_j)} - \frac{\gamma^2 n(q_k) n(\bar{q}_k)}{1 + \gamma n(q_k) + \gamma n(\bar{q}_k)} \right]. \end{aligned} \tag{A.6}$$

References

1) G.F. Mazenko and S. Yip, in: Statistical Mechanics, part B: Time-Dependent Processes, B.J. Berne, ed. (Plenum Press, New York, 1977) Chap. 4.
2) C.D. Boley and J.B. Smith, Phys. Rev. **A12** (1975) 661.
3) O.T. Valls, G.F. Mazenko and H. Gould, Phys. Rev. **B18** (1978) 263.
4) E.A. Uehling and G.E. Uhlenbeck, Phys. Rev. **43** (1933) 552.
5) N.N. Bogoliubov and K.P. Gurov, Zh. Eksp. i Teor. Fiz. **17** (1947) 614.
6) E.P. Wigner, Phys. Rev. **40** (1932) 749.
7) A.L. Fetter and J.D. Walecka, Quantum Theory of Many-Particle Systems (McGraw-Hill, New York, 1971).
8) L.D. Landau, Zh. Eksp. i Teor. Fiz. **7** (1937) 203; also in: Collected Papers of L.D. Landau, D. ter Haar, ed. (Pergamon Press, Oxford, 1965) p. 163.
9) A.Z. Akcasu and J.J. Duderstadt, Phys. Rev. **188** (1969) 479.
10) D. Forster and P.C. Martin, Phys. Rev. **A2** (1970) 1575.
11) S.T. Choh (and G.E. Uhlenbeck), Ph.D. Diss., University of Michigan (1958).
12) C.D. Boley and R.C. Desai, Phys. Rev. **A7** (1973) 1700.